Dynamic measurements and wettability phenomena in mesoporous anodic films prepared on 1050 and 2024T3 aluminium alloys

Kévin Giffard [a], Laurent Arurault [b, *], Christine Blanc [c]

[a] MECAPROTEC Industries, 34 Boulevard de Joffrery, 31600 Muret, France
[b] CIRIMAT, Université de Toulouse, CNRS, INPT, UPS, Université Toulouse 3 Paul Sabatier, Bât. CIRIMAT, 118 route de Narbonne, 31062 Toulouse cedex 9, France
[c] CIRIMAT, Université de Toulouse, CNRS, INPT, UPS, ENSIACET, 4 allée Emile Monso BP 44362, 31030 Toulouse cedex 4, France

ABSTRACT

The wettability of mesoporous anodic films has until now been a parameter rarely studied although it remains crucial especially for sealing treatment following anodising. Wettability measurement is in fact complex as it depends on a number of process parameters relating to the three phases (mesoporous anodic film, deposited liquid and ambient gas). In the present study, an innovative experimental approach was first adopted involving measuring the characteristics of a deposited water drop (contact angle, chord length and height of the drop) in relation to time. Following this, a flow balance allowed the amount of water having infiltrated the mesopores to be determined for two types of anodic film, one tortuous (on an AA 2024T3 substrate), the other not (on an AA 1050 substrate). On the basis of models already available in the literature, a phenomenological mechanism (spreading, penetration and evaporation) was finally proposed and discussed especially with respect to the tortuosity and prior drying of mesoporous anodic films.

1. Introduction

Evaluating wettability by measuring the contact angle is a complex characterisation as it depends on several process parameters [1,2]. Indeed, the shape a drop of solvent takes when deposited on a substrate results from an equilibrium between the intermolecular interactions present on the three solid—liquid, liquid—gas and gas—solid interfaces. Thus, as far as the solid substrate is concerned, the contact angle is influenced by its roughness, its porosity and the air that may be trapped in the pores, its chemical nature and its hydration, its surface charges and temperature. Moreover, the nature, the charges and temperature of the liquid on the one hand and the nature, the charges and temperature of the gas on the other, also influence the contact angle.

Few studies [3—10] have been devoted to the characterisation of wettability of porous anodic films, coated or not, and those works that do exist only consider the influence of a few parameters at a time. Again, most studies of wettability on anodic films implement static contact angle measurements using a goniometer. A drop of

solvent is then deposited and measurement of the contact angle at the triple point is made as soon as the liquid comes into contact with the surface (Fig. 1). Young's law (Eq. (1)) then connects the contact angle (θ) to the surface tensions (γ) on the three solid/liquid, liquid/gas and solid/gas interfaces. However, this law is valid in the case of partial wetting and assumes that the energies on the three interfaces are in thermodynamic equilibrium, the second condition only holding good in the case of a perfect solid, free of roughness.

$$\gamma_{sg} = \gamma_{sl} + \gamma_{gl} \cos \theta \qquad (1)$$

with: θ = static contact angle

γ_{sg} = surface tension at the solid/gas interface
γ_{lg} = surface tension at the liquid/gas interface
γ_{sl} = surface tension at the solid/liquid interface

As an anodic film cannot, if only due to its porosity, be perfect, the static mode thus appears to be largely inadequate in this case as the drop is not in equilibrium and part of the data would as a result be lost. Washburn's technique [1,7] in part alleviates this drawback. The technique used in the present study is innovative as standing
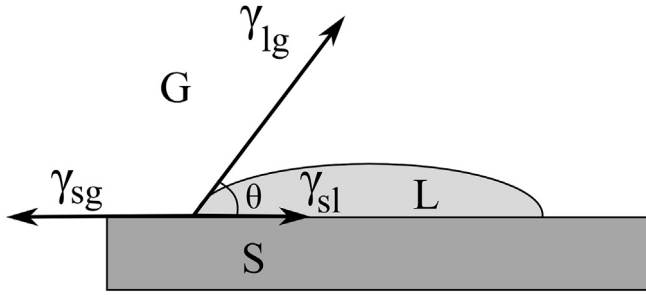
Fig. 1. Diagram of a drop of liquid L in equilibrium with a solid surface S and a gaseous phase G.

midway between the goniometric method and the Washburn method, involving depositing a drop and measuring the contact angle over time. It will thus be possible to monitor penetration of the solvent into the porous anodic film, especially in the first instants, before the drop reaches an "equilibrium" with the surface. The present study's objective will finally be to determine the various phenomena involved in the wettability of water on mesoporous anodic films prepared in sulphuric acid solution on 1 mm rolled AA 1050 and AA 2024T3 substrates. These results will be useful in understanding the sealing phenomena of these anodic films.

2. Material and methods

Aluminium alloy 1050A (99.5% Al, <0.40% Fe, <0.25% Si and <0.05% Cu, wt%) and AA 2024 (90.7 < Al < 94.7%, 3.8 < Cu < 4.9%, 1.2 < Mg < 1.8%, 0.3 < Mn < 0.9%, <0.50% Fe, <0.50% Si, <0.25% Zn, <0.15% Ti, 0.10% Cr, wt%) were both used as two different types of substrates: 1050 (rolled; thickness of the sheet = 1 mm) and 2024 T3 (rolled; thickness of the sheet = 1 mm). In addition, all chemical compounds used were analytical grade, while aqueous electrolyte solutions were obtained using deionised water.

2.1. Surface preparation

The surface preparation process principally involved three successive steps: degreasing, etching and finally anodising.

Aluminium alloy sheet ($50 \times 50 \times 1$ mm of treated surface) was first degreased using acetone $(CH_3)_2CO$ before being placed for 20 min in an aqueous bath (pH ≈ 9; 60 ± 2 °C) containing sodium tripolyphosphate $Na_5P_3O_{10}$ (40 g L^{-1}) and sodium tetraborate (borax) $Na_2B_4O_7 \cdot 10H_2O$ (40 g L^{-1}), and then etched in aqueous sulpho-nitro-ferric solution (pH ≈ 2; 25 ± 5 °C) for 5 min. The sample was immediately rinsed with distilled water after each step, carried out at ambient temperature.

The sample was then used as an anode and a lead plate ($56 \times 56 \times 1$ mm of immersed surface) as a counter-electrode in an electrochemical cell containing stirred aqueous H_2SO_4 bath (200 rpm; 200 g/L, i.e. 2.039 mol/L), thermostated using Huber CC2 cryostat; The bath temperature was 19.0 ± 0.5 °C and 20.0 ± 0.5 °C for AA1050 and AA2024T3 respectively, so as to precisely obtain the same film thickness on both substrates. Anodising was conducted in potentiostatic mode (TDK lambda GEN 300-S) using an initial voltage slope (3 V/min) up to the rated voltage (16 V) applied for 10min (AA1050) or 15 min (AA 2024T3). Following anodising, the sample was immediately rinsed with distilled water. In these operating conditions, the thickness of the resulting anodic films is typically 5.0 ± 0.5 µm [11] whatever the substrate used, while the mean pore diameter is 10 ± 4 nm (Fig. 2a) [12] and 8 ± 2 nm

(Fig. 2b) [12] for 1 mm rolled substrates AA 1050 and AA 2024 respectively.

2.2. Characterisations

Contact angle measurements were made using a DIGIDROP Fast 60 GBX contact angle meter. Ultrapure water with resistivity close to 18 MΩ was used as a solvent in all the measurements. GBX glass syringes with a 0.71 mm diameter Teflon needle were used to deposit the drops. The equipment was controlled by the WinDrop ++ software to deposit controlled volume drops (4.1 ± 0.3 µL) and acquire images by 40 ms increments.

Faced with the large number of process parameters influencing the contact angle measurement, it was first decided to restrict their number by choosing invariant parameters.

Firstly, concerning the liquid deposited, the choice went in favour of water as this is the solvent used for sealing baths. Water has both a high dielectric constant ε and dipole moment µ (ε = 80; µ = 1.85 Debye) but a high surface tension γ ($\gamma_{water} = 73$ mN m^{-1}), which is unfavourable to interactions with alumina and leads to usually high contact angles (80° [3], 85° [9] on compact flat alumina).

Concerning the gaseous environment, ideally the various characteristics have to be strictly controlled. Sobczak et al. [13] thus insisted on the influence of the nature of the gaseous environment and its partial pressure in oxygen that may in particular lead to oxidation of the substrate or the drop at high temperature. Song et al. [14] worked in a controlled environment, highlighting the importance of maintaining controlled temperature (T ± 1 °C) as well as controlled relative humidity (RH ± 1%). Indeed, the volume of liquid transferred in the vapour phase (V_{evap}), meaning the volume that evaporates into the surrounding gas, depends on its temperature, pressure and hygrometry conditions. The liquid will tend to evaporate more readily when its partial pressure contained in the gas is low; in other words, in the case of water and air, as far as the relative humidity is low or the air is "dry". Control over these parameters is essential to keep constant evaporation of the drop and measure the contact angles in repeatable manner. But in practice these parameters are hard to control unless when working in an enclosed chamber. In the present study, the measurements were not made in a confined chamber but in an air conditioned room. In such conditions, the temperature and degree of humidity remained relatively constant from one series of measurements to another, between 21 and 23 °C and 45 and 60% respectively.

Concerning the anodic film, special attention was given to prior drying of the film that is especially important as it significantly influences wettability [15,16]. Indeed, penetration of the liquid (here water) will be modified according to whether the pores are initially filled with water or air. The anodic films applied in the literature are generally dried under a flow of nitrogen [5] or placed in an oven for 1—6 h at a temperature of 70 °C—100 °C [3,7]. In the present study, the films were placed in an air drier connected to a primary vacuum pump for 15 min, then in an oven at 60 °C for 30 min. This procedure allows for dehydration of a proportion of the physisorbed water, while avoiding possible sealing that can arise in an oven at 100 °C.

The technique employed in the present study involves depositing a drop and measuring the contact angle over time. Using this method, the contact angle is first determined, but analysis of the images at a given instant (t) also allows the chord (c) to be measured as well as the height of the drop (h) expressing how it spreads over the surface (Fig. 3). The volume of the drop over time is also accessible using measurements of the chord and the height of the drop, and calculating the radius of the sphere (R_d) formed by
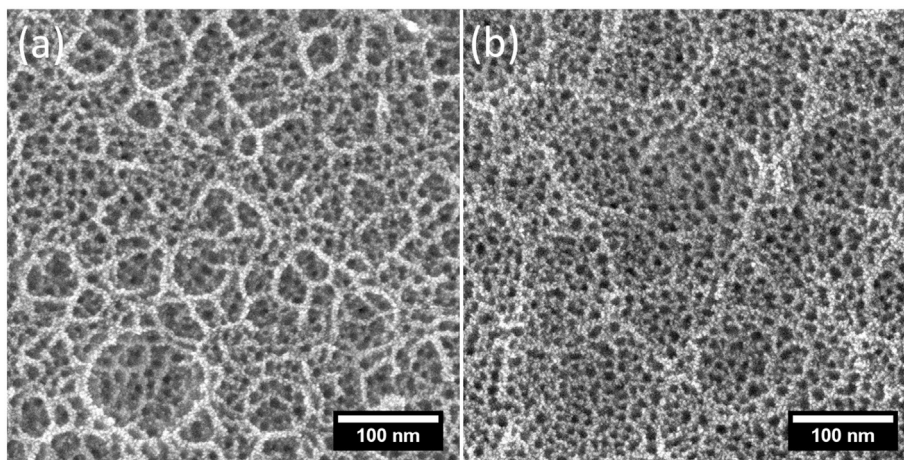
Fig. 2. FEG-SEM surface views [12] of the mesoporous anodic films prepared on 1 mm rolled substrates (a) AA 1050 and (b) AA 2024 T3.
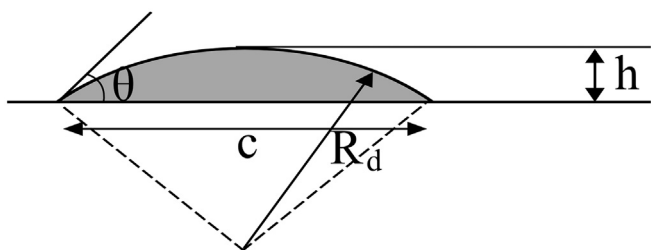

Fig. 3. Diagram representing the characteristic lengths of a drop considered as a spherical cap.

the drop. All these parameters allow penetration of the solvent into the porous anodic film to be monitored.

In addition, the mean arithmetic roughness (Ra) was measured using a Zygo© optical interferometer placed on an air cushion table and controlled by the Metropro 7.12.0 software combined with the microscope application. Each value for Ra shown (Appendix) corresponds to the mean of 15 measurements.

3. Results and discussion

Preliminary verifications proved that measurements were made in satisfactory conditions (Appendix). Notably, it was checked that the syringe deposits drops in repeatable fashion to have the correct volume every time (Appendix A1), meaning relevant flow balances could be established. In addition, the drop did not deform as the Bond (or Eötvös) number (B_0) remained less than 1 (Figs. A2 and A3 in Appendix A2) and the direction of observation, along the direction of rolling of the substrate or perpendicularly, had no influence on the contact angle (Figs. A4 and A5), although all the measurements were always made in the perpendicular direction.

3.1. "Apparent drop" contact angle, chord, height and volume

The contact angle on anodic film on substrate AA 1050 is initially equal to 17° (Fig. 4) then decreases monotonously to 14°. The height curve shows similar shape, i.e. the height falls rapidly in the first seconds, corresponding to the contact of the drop with the anodic film. Then there is a gradual decrease in height, but with a shallower slope. The chord value, initially equal to 4.8 mm, suddenly increases during the first 4 s to reach a maximum of 4.9 mm

indicating substantial spreading. After 4 s, a reduction in the chord is observed, this period being termed the "receding phase".

Fig. 5 shows that evolution of wettability on anodic film on substrate AA 2024T3 is similar, although with a maximum chord slightly greater (5.3 mm), and a reduction of the chord as from 20 s. The contact angle and the drop height have a similar appearance, with a rapid decrease in the first seconds and then a lower one.

Two assumptions can then be posited to explain this reduction in the chord:

- either it is associated with an evaporation phenomenon,
- or it results from penetration of the liquid into the pores.

The "apparent drop" volume, meaning the "spherical cap" remaining apparent on the anodic film (Fig. 3), is calculated using eqs (2) and (3). How it changes in relation to time is shown in Fig. 6. It can be especially noted in Fig. 6 that, even though a water volume of 4 μL was initially dropped, both curves started from 3.2 to 3.3 μL. Indeed, on a porous material such as anodic films, the whole dropped volume does not have time to be fully transferred to the film and a portion of the volume remains attached to the syringe. Statistical evaluation of the volume that remains hanging on, was carried out and provided a mean value equal to 0.56 μL. The volume hanging onto the syringe is not involved in measurements showed in Fig. 6.

$$V = h^2(3R_g - h) \cdot \pi/3 \qquad (2)$$

$$R_g = \left(c^2/8h\right) + (h/2) \qquad (3)$$

with V = drop volume, h = drop height, c = drop chord and R_d = radius of the sphere formed by the drop.

The apparent drop volume vs time curve corresponding to the anodic film on substrate AA 1050 (Fig 6) shows a break in slope illustrative of gradients of reduction of the "apparent drop". The first regime corresponds to a rapid (0.15 μL/s) and significant disappearance in volume, while the second regime is associated with a much shallower slope (0.005 μL/s). These observations can be seen to reflect the penetration of the solvent into the anodic film (first regime), while the second regime may correspond to an evaporation phenomenon. Thus, out of the drop's initial volume of 4 μL, there remains about 2.5 μL after 120 s, meaning after measurement. Out of the 1.5 μL reduction, 1 μL would seem to be accounted for by the solvent's penetration into the film, divided
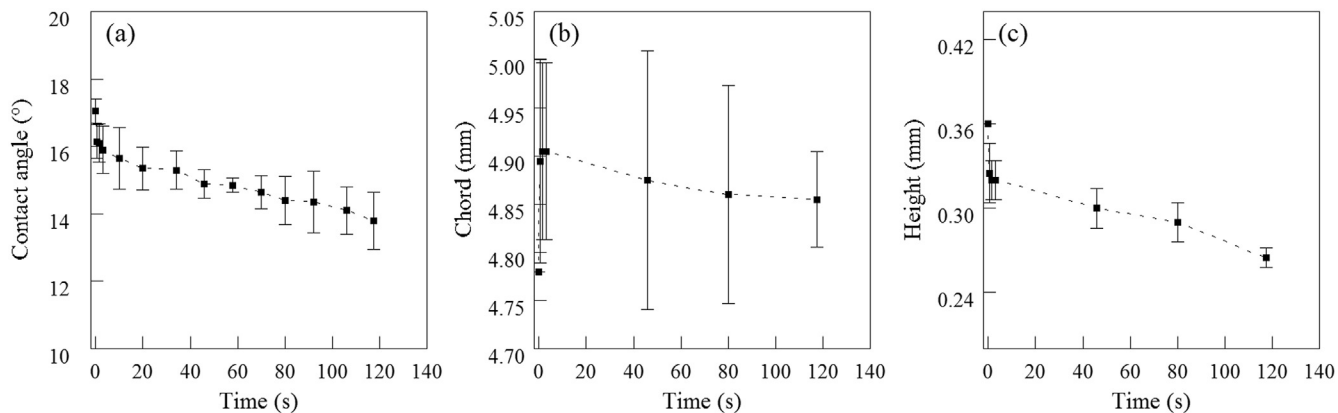
Fig. 4. Evolution of the contact angle, chord and height over time on an anodic film (5 μm) formed on 1 mm rolled substrate AA 1050.
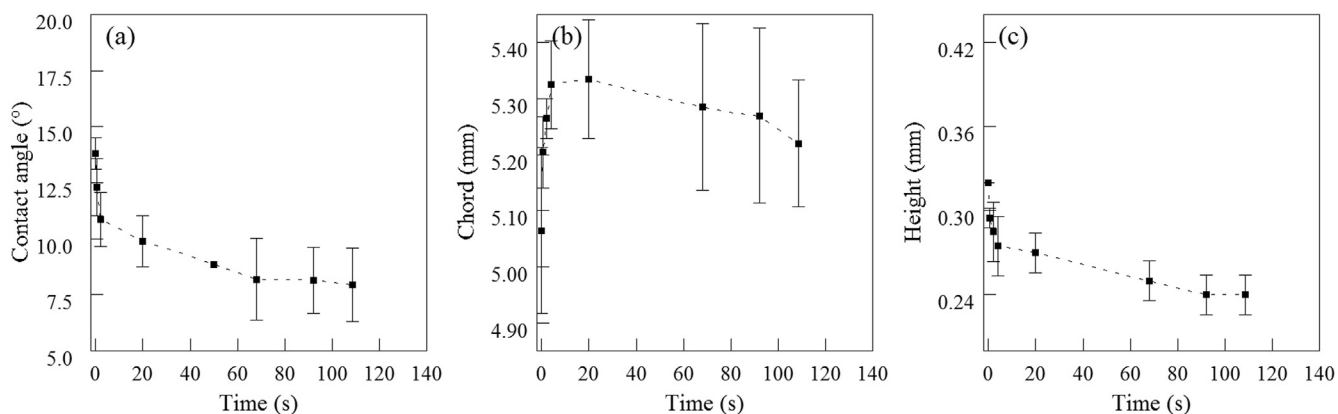

Fig. 5. Evolution of the contact angle, chord and height over time on an anodic film (5 μm) formed on 1 mm rolled substrate AA 2024T3.
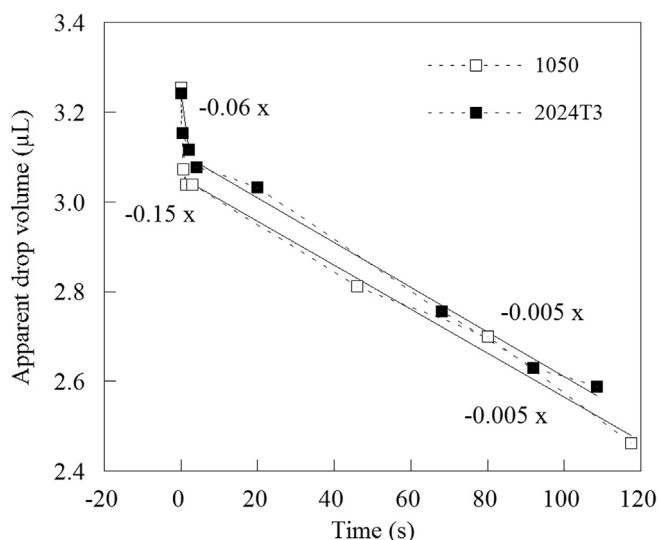

Fig. 6. Evolution of the mean "apparent drop" volume over time on anodic film (5 μm) formed on 1 mm rolled substrates AA 1050 and AA 2024.

between 0.7 μL (i.e. 70% of the volume reduction) as soon as the drop comes into contact with the anodic film and the remainder during the first second. The kinetics of the water's penetration into the film thus seems to be extremely rapid since the break in slope

arises as from t = 1 s, leading to the second regime (evaporation) during which 0.5 μL disappears.

The curve corresponding to the anodic film on substrate AA 2024T3 (Fig 6) has a very similar appearance to that corresponding to substrate AA 1050. The slope of the second regime is thus identical (0.005 μL/s) to that obtained previously, while conversely the slope corresponding to the first regime is much shallower (0.06 μL/s instead of 0.15 μL/s). There would thus appear to be a difference in the solvent's penetration into the anodic film (first regime), while the second regime corresponding to the evaporation phenomenon remains largely unchanged.

3.2. Flow balance and penetration of water into the porosity

An additional flow balance allows the reduction in the volume of solvent to be quantified more precisely, considering that the "apparent drop" volume over time is defined by (Eq. (4)):

$$V_{(t)} = V_0 - V_{evap(t)} - V_{dim(t)} \tag{4}$$

with: V_0 = initial drop volume (4 μL)

V_{evap} = volume transferred to the vapour phase (here air) by evaporation

V_{dim} = reduction in the drop volume

Thus, the reduction in volume (V_{dim}), in other words the volume that can a priori be considered to have penetrated the anodic film, is given by the equation:

$$V_{dim(t)} = V_0 - V_{evap(t)} - V_{(t)} \qquad (5)$$

A statistical study was then conducted depositing a drop on anodic films on 1 mm rolled substrates AA 1050 and AA 2024. For each type of film, measurement was repeated ten times on two different samples, keeping the drops sufficiently far apart to avoid inter-drop interactions, which gave the mean volume of loss at t = 2s (considering the share of evaporation to be negligible in relation to penetration given the timescale). In addition, the pore space volume present in the film, accessible to the water drop, was evaluated, considering a model of cylindrical pores and assuming that initially the water can only access the volume of porosity present directly under the drop. To do so, the area of the drop/anodic film (A_{ls}) interface was calculated from the drop chords in accordance with Eq (6).

$$A_{ls} = \pi \cdot (C/2)^2 \qquad (6)$$

Fig. 7 allows the volume of solvent that can be reckoned a priori to penetrate the anodic film in relation to the volume of porosity available under the drop to be compared for films formed on the two substrates considered. This final volumic balance took into account the volume hanging onto the syringe, unlike the measurements previously showed in Fig. 6. To sum up, the mean volume of reduction associated with the anodic film on 1 mm rolled substrate AA 1050 is equal to 0.44 ± 0.15 μL, while it is equal to 0.26 ± 0.14 μL on the anodic film on substrate AA 2024 for an identical calculated porosity volume V_p under the area of the drop.

In both cases, and a priori somewhat surprisingly, the volume of solvent penetrating the anodic film is greater than the volume of porosity available under the drop calculated on the basis of a cylindrical geometry of the pores. Furthermore, although the mean
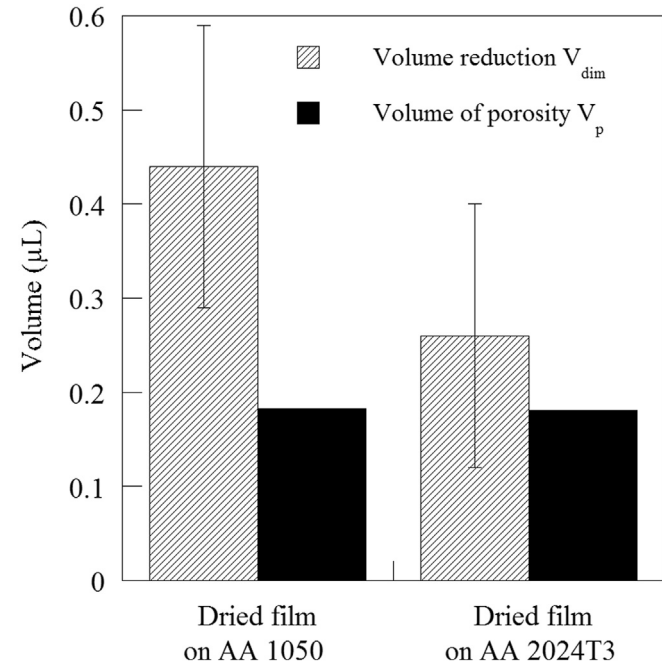
porosity volumes available under the drop are identical on substrates AA 1050 and AA 2024 (on the basis of a model of cylindrical pores), penetration seems to be more significant in the film on substrate AA 1050 as the reduction in volume is greater there (0.44 ± 0.15 μL as against 0.26 ± 0.14 μL).

Table 1 [12] first shows that the surface charges are identical (in the order of +50 mV) to the pH of the drop (ultrapure water, pH = 5.3) for these two anodic films. Furthermore, Table 1 shows that the roughness values for anodic films (5 μm) on both substrates are close and that the maximum chords (and thus maximum spreading) are similar, as also porosity (15 ± 3%) [12]. However, the tortuosity values could explain the differences in penetration, since when taking into account this parameter, the volume available under the drop is greater than with the cylindrical pores model. The difference in porosity available under the drop due to tortuosity can thus be a first explanatory factor, but would not fully explain why, in both cases and above all in the case of substrate AA 1050, the volume of solvent penetrating the anodic film is greater than the volume of porosity available under the drop. Indeed, tortuosity is greater for the substrate AA 2024 than for the substrate AA 1050 (1.43 instead of 0.96 respectively [12]) while penetration into the anodic film on AA 2024 substrate is less significant. It is therefore appropriate to look for other possible phenomena, as with the example of formation of a precursor film.

3.3. Formation of the precursor film

A first hypothesis could be based on the fact that the water penetrates the anodic film and occupies the entire volume available under the drop, both in the film on substrate AA 1050 and the film on substrate AA 2024. This assumption appears somewhat unlikely in so far as there is a greater excess volume (0.44 ± 0.15 μL) in the film on substrate AA 1050 as compared with that on substrate AA 2024 (0.26 ± 0.14 μL), while the former film has cylindrical pores and tortuosity (and thus a pore space volume) less than those of the film on substrate AA 2024.

If the solvent penetrates the entire volume available under the drop in the film on alloy AA 1050, the following hypothesis would involve an additional spreading hitherto not taken into account. W. B. Hardy [17] showed for the first time that the deposition of a drop on a surface may lead to the formation of an invisible precursor film of liquid that spreads rapidly in all directions, leading to a drop in surface tension. While it proves difficult here to determine the surface tension, Hardy [17] proved the existence of this film by performing measurements of the static coefficient of friction. Following that, Bormashenko et al. [18] proved that the formation of such a film occurred from the triple line of the drop, on a rough surface, by making observations on an environmental SEM. In the present study, the creation of a film of water of this type on the anodic film would probably allow for an explanation of how (especially on substrate AA 1050) the reduction in the drop volume observed (0.44 ± 0.15 μL) is greater than the available porosity volume (0.18 μL) under the drop.

Additional measurements were made in order to highlight the possible existence of spreading of such a precursor film. Hitherto, all measurements were made on previously dried anodic films. This time, such additional measurements were performed on an anodic film formed on a non-dried, rolled substrate AA 1050, meaning in other words on a film where porosity is already filled with water.

Fig. 8 shows that the mean volume of reduction in liquid (0.26 ± 0.14 μL) on non-dried film corresponds exactly to the excess volume (0.44 − 0.18 = 0.26 μL) that did not penetrate on the dried film on substrate AA 1050. As the porosity of the non-dried anodic film is a priori filled with water, this reduction in volume (in the order of 65%) could thus be related to the spreading of a precursor

Fig. 7. Mean reduction in the drop volume (V_{dim}) at t = 2 s on anodic film (5 μm) prepared on 1 mm rolled substrates AA 1050 and AA 2024. Comparison with the volume of porosity (V_p) available in the anodic film under the surface area of the drop.

Table 1
Zeta potential, roughness, chord of the drop, mean pore diameter and porosity and tortuosity of the anodic films (5 μm) on 1 mm rolled substrates AA 1050 and AA 2024T3 [12].

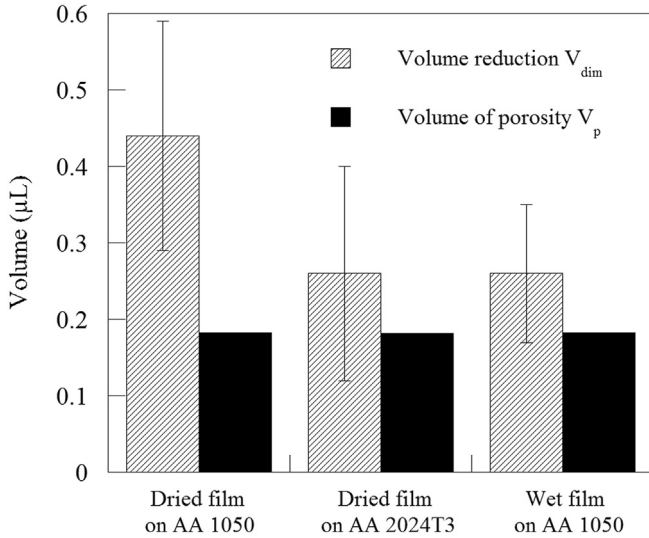| Substrate	1 mm rolled AA 1050	1 mm rolled AA 2024T3
Zeta potential (mV) at pH 5.3 [12]	50 ± 1	50 ± 3
Arithmetic roughness Ra (μm) [12]	0.33 ± 0.03	0.34 ± 0.12
Mean pore diameter (nm) [12]	10 ± 4 nm	8 ± 2 nm
Porosity (%) [12]	15 ± 3	15 ± 3
Tortuosity [12]	0.96	1.43
Chord max. (mm)	4.9	5.3

Fig. 8. Mean reduction in the drop volume (V_{dim}) at t = 2 s on dried anodic film (5 μm) on 1 mm rolled substrates AA 1050 and AA 2024 and on non-dried anodic film on 1 mm rolled substrate AA 1050. Comparison with the volume of porosity (V_p) available in the anodic film under the surface area of the drop.

film. These results also show that the influence of tortuosity is negligible for the anodic film on substrate AA 1050, contrary to the case of anodic film on substrate AA 2024.

Moreover, Fig. 8 also shows that the mean volumes of loss on films on dried substrate AA 2024 and on non-dried substrate AA 1050 are equal. It can thus be considered that the loss of solvent on film on substrate AA 2024 can also be only associated with the creation and spreading of this invisible film. This situation is all the more plausible in that the two films have similar charges and roughness (Table 1); however, the tortuosity of the film on substrate 2024 is the more pronounced (1.43) of the two [12], which probably further limits penetration of water in the case of this substrate as compared with substrate AA 1050.

Calculation of the thickness of the precursor film, considering that the excess volume (0.26 μL) spreads over the entire surface of the coupon (25 cm^2), gives a value of 100 nm. This result seems to fit in with the fact that this precursor film is invisible.

3.4. Influence of the film thickness on the contact angle

Ran et al. [4] devised films in one stage in H_3PO_4-H_2O-C_2H_5OH, followed by a treatment of pore opening in H_3PO_4 over different time periods. They notably reported that as from 1.7 μm, the thickness of the anodic film has very little influence on the contact angle. Conversely, Buijnsters et al. [3] highlighted an evolution in the contact angle for anodic films thicker than 5 μm, produced by double anodising in a phosphoric acid medium (10 or 5 or 1 wt%;

T = 0 °C; 160–195 V; 15–300 min) followed by a treatment of pore opening in a phosphoric medium (5% mass; T = 30 °C; 60–150 min).

Given such a contradiction and in order to verify the incorporation of water for variable shape factors (σ), contact angle measurements were made in relation to time (0–100 s) on anodic films with a thickness of between 2 and 15 μm (Fig. 9) prepared on substrate AA 1050, then dried beforehand. Fig. 10 highlights a quasi-linear evolution of the initial contact angle (at t = 0) with the thickness of the anodic film. On these anodic films, made from the same material batch and characterised on the same day, only the thickness changes, and thus only the volume of porosity available evolves (0.07 μL (e_{film} = 2 μm); 0.18 μL (e_{film} = 5 μm); 0.55 μL (e_{film} = 15 μm)). Thus, the reduction in the contact angle (at t = 0) observed (25° (e_{film} = 2 μm); 21° (e_{film} = 5 μm); 14° (e_{film} = 15 μm)) can be attributed solely to penetration of the drop in the increasingly thick (from 2 to 15 μm) anodic film. Indeed, as the roughness, porosity and the chemical nature are the same for the three films, the precursor film would a priori be identical in each case; the reduction in the contact angle would thus correspond to a volume of water incorporated that increases with the thickness of the anodic film, and thus the pore space volume available under the drop.

As for later reductions (up to 23° (e_{film} = 2 μm), 18° (e_{film} = 5 μm), 12° (e_{film} = 15 μm) after 100 s) in relation to time (Fig. 9), they correspond in each of these cases to the evaporation
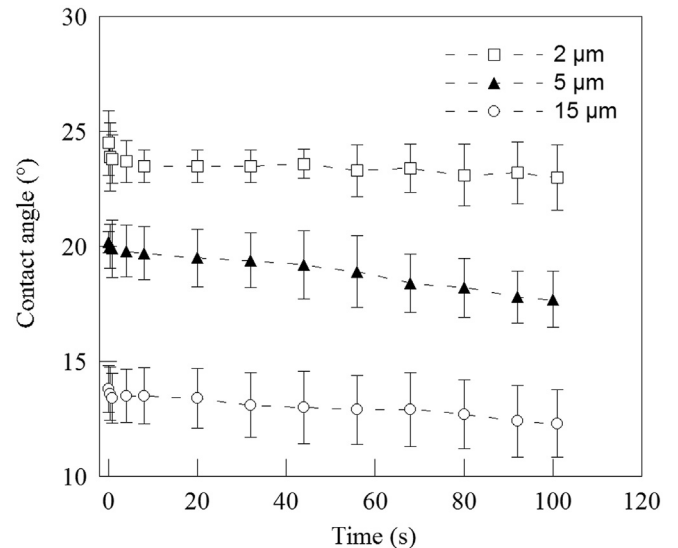

Fig. 9. Evolution over time of the contact angle on dried anodic films with varying thickness (2, 5, 15 μm) prepared on 1 mm rolled substrate AA 1050.
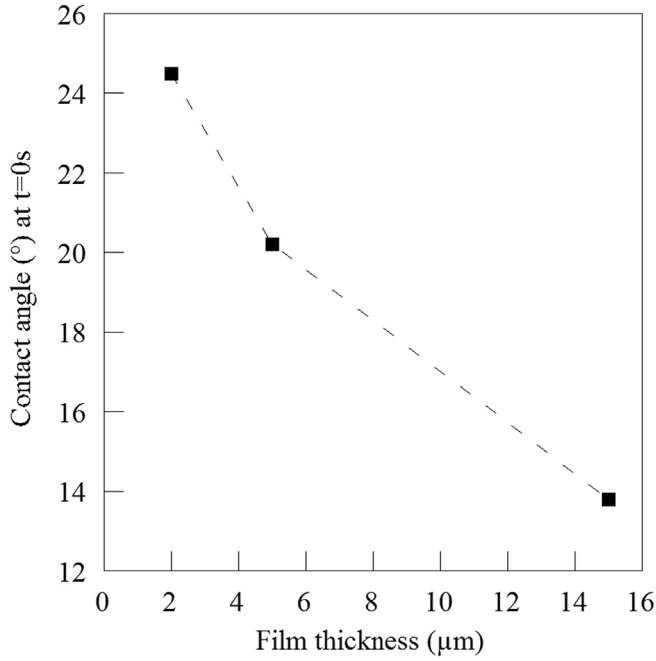
Fig. 10. Evolution of the initial contact angle in relation to the thickness of the anodic film.

phenomenon, that varies significantly in relation to the drop volume, and the temperature (21–23 °C) and humidity (45–60%) variations of the air conditioned room.

3.5. Discussion around existing infiltration models

The wettability of porous materials is usually modelled using Wenzel or Cassie-Baxter equations. The Wenzel contact angle (θ_W) first integrates the contribution of surface roughness in relation to Young's contact angle (θ_Y) via a roughness factor r (Eq. (7)). This model, in which the solvent clings to the roughness, would seem suitable to describe the case where penetration of the solvent into the pores is complete [5]. Conversely, the Cassie-Baxter model is more appropriate to describe the case where the solvent does not penetrate the asperities or the porosity of the solid, but remains on the surface. This second model considers the effect of a chemical heterogeneity of the surface and allows calculation of a global contact angle θ_{CB} corresponding to the combination of contributions of the various contact angles (Eq. (8)).

$$\cos \theta_W = r\cos \theta_Y \tag{7}$$

$$\cos \theta_{CB} = f(\cos \theta_Y + 1) - 1 \tag{8}$$

with f the surface fraction of solid wetted by the liquid.

For the present study, the Wenzel model would seem to be appropriate to describe the wettability of the anodic film formed on substrate AA 1050, the results having highlighted complete penetration of the water into the porosity. However, the Cassie-Baxter model meanwhile may appear better suited to describe wettability of the film on substrate AA 2024.

Raspal et al. [5] meanwhile followed evolution of the contact angle in relation to the pore diameter and sought to model their experimental data using these two models. Their results (using water, ethylene glycol or aniline liquids) finally showed that the Cassie-Baxter and Wenzel models quickly reach their limits,

especially when it comes to describing intermediate cases involving incomplete penetration of the liquid into the pores.

Other models have thus been developed [19]. In particular, Laplace's model allows the case of partial filling of the pores of an initially empty (in our case previously dried) anodic film [3] to be addressed and especially for the height (h) of liquid that infiltrated the pores to be evaluated (Eq. (9)). This model is firmly based on physical principles, taking into account capillarity force (Eq. (10)) that counterbalances the pressure force exerted by the air in the pores and creates a real obstacle to penetration of the solvent into the pores (the gravitational force involving the weight of the drop being considered negligible as $B_0 < 1$ (Appendix A2)). Nevertheless, Raspal et al. [5] reported that, in the same way as the Wenzel model, the Laplace model overestimates the rate of penetration, especially for low pore diameters. On the basis of the Laplace model, it then proved possible to evaluate quantitatively the penetration of water into the anodic film supported on substrate AA 1050. Indeed, the model (Eq. (9)) predicts penetration (h) in the order of 97% of the length of the pores (with $e_{film} = 5$ µm, d = 10 nm), which would indicate complete penetration of the solvent in this instance.

$$h = 4 \cdot e_{film} \cdot \gamma \cdot \cos \theta / (P_0 \cdot d + 4 \cdot \gamma \cdot \cos \theta) \tag{9}$$

$$F_c = \pi \cdot \gamma \cdot d \cdot \cos \theta \tag{10}$$

with: γ: surface tension of the water

d: pore diameter
θ: Young's contact angle
e_{film}: thickness of the anodic film
P_0: atmospheric pressure

Hilpert and Ben David [20] meanwhile proposed a model of infiltration in three phases of a drop resting on an ideal porous medium made up of empty, rectilinear and non-interconnected tubes:

- The first phase (Increasing Drawing Area (IDA)) involves increasing the chord and reducing the contact angle as far as t = t_a. The experimental data on films on substrates AA 1050 and AA 2024 concur with these first events that occur up to t = 4 s (Fig. 4). Indeed, the chord increases, going from 4.78 to 4.91 mm on film on substrate AA 1050 and from 5.07 to 5.33 mm on film on substrate AA 2024. The contact angle also diminishes down to t = 4 s on both films.
- During the second phase (Constant Drawing Area (CDA)), the chord is constant while the height and contact angle diminish. The present experimental data indeed highlight a reduction in the contact angle combined with a reduction in the drop height, which goes from 0.33 to 0.27 mm on film on substrate AA 1050, and from 0.27 to 0.24 mm on film on substrate AA 2024. In addition, as with the model, the experimental chord on anodic films seems constant, taking into account measurement uncertainties.
- Finally, the third phase (Decreasing Drawing Area (DDA)) involves reducing the chord and the height until the drop completely disappears. The maximum acquisition time for the experiment (120 s) was not sufficient to record all of this third phase.

Changes in the contact angle, the chord and height observed experimentally thus seem to comply with the phenomenological model of Hilpert and Ben David [20]. The IDA phase would correspond to the spreading of the precursor film and above all

penetration (near total into the film on substrate AA 1050 and slight on substrate AA 2024T3) of water into the porosity present under the initial drop. Meanwhile, the CDA and DDA phases would seem to relate to the evaporation of the residual spherical cap present on the anodic film.

4. Conclusions

The wettability of a mesoporous anodic film is a complex and hitherto rarely studied characteristic. In the present work, it was studied using an innovative method (at an intermediate position between the goniometric method and the Washburn method) that involved measurements of the contact angle over time in strictly controlled operating conditions. The results show that the water penetrates rapidly into the entire volume (97% according to the Laplace model) of ordered mesoporosity ($\varnothing_{pores} = 10 \pm 4$ nm) available in the anodic film prepared on previously dried 1 mm rolled substrate AA 1050. However, penetration of the water would seem to be limited in the anodic film ($\varnothing_{pores} = 8 \pm 2$ nm) formed on 1 mm rolled substrate AA 2024 previously dried. The significant tortuosity (1.43 instead of 0.96 for AA 1050) would in this case be responsible, by preventing the evacuation of the air trapped in the mesopores. Detailed analysis of all the results shows that there must first have been the formation of a precursor film (about 100 nm thick), then incorporation of the water into the porosity (in the case of substrate AA 1050 and not that of 1 mm rolled substrate AA 2024), and finally gradual evaporation of the spherical cap of superficial residual water, these results being very much in line with the phenomenological model previously proposed by Hilpert and Ben David [20]. One interesting perspective would in the future be to use not water but a low energy liquid like dimethylformamide (DMF) ($\gamma_{DMF} = 25$ mN m^{-1}), whose interaction with the alumina is energetically more favourable than with water ($\gamma_{water} = 73$ mN m^{-1}). It would also be interesting to perform measurements of the static coefficient of friction so as to corroborate the existence of the precursor film on these porous anodic films.

Appendices

Appendix A1 Drop volume

Preliminary measurements were made in order to check that the volume of the drop deposited is equivalent to the desired theoretical volume as set by the goniometer. A drop is deposited on a glass slide then weighed using a precision balance. The procedure is repeated ten times for each volume (1; 4; 6; 9 µL). The mean and the low standard deviation, as shown on Fig. A1, indicate that the machine deposits the correct volume in a reproducible manner.
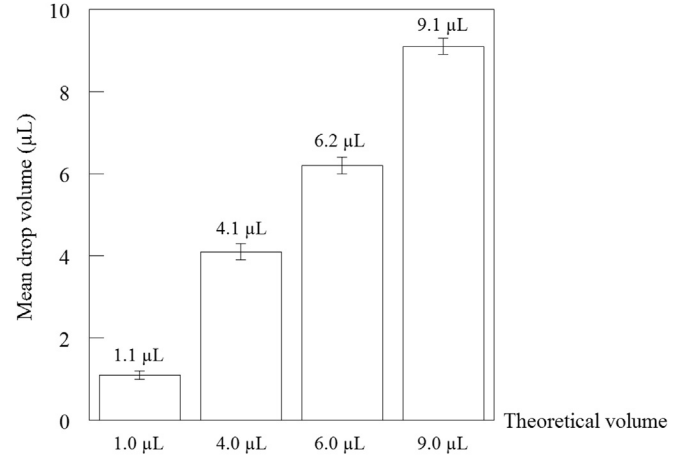

Fig. A1. Real mean drop volume deposited by the goniometer on thin glass slide for different theoretical volumes.

Appendix A2 Drop shape

Preliminary measurements also involved verifying the shape of the drop via the criterion known as the Bond number B_0. This number, defined by Eq. (11), allows the significance of surface tension forces to be determined in relation to gravity. Typically, a value lower than one indicates that the surface tension predominates. Alternatively, if the radius of the drop R_d is less than the capillary length L_c (Eq. (12)) then the capillary effects will win out over the gravity effects. Conversely, if R_d is greater than L_c, then gravity effects will predominate, the drop will no longer have a spherical shape and calculations on the drop's volume will no longer be relevant. In the case of a drop of ultrapure water, the capillary length equals $L_c = 2.71$ mm. Thus, drops of varying volume (0.5–9 µL) were deposited on 1 mm rolled substrate AA 1050, simply degreased using acetone ($CH_3)_2CO$. Fig. A2 shows that the drop was neither flattened nor deformed and Fig. A3 shows that $R_d < L_c$ and $B_0 < 1$. The measurements are thus valid for the entire range of volumes in the study.

$$B_0 = (d \cdot g \cdot l)/\gamma \sim R_d{}^2 \Big/ \left(L_c{}^2 \right) \tag{11}$$

with: d: density of the liquid

g: acceleration due to gravity
L: drop radius
γ: surface tension

$$L_c = [\gamma/(d \cdot g)]^{1/2} \tag{12}$$

Substrates AA 1050 and AA 2024T3 used in the study have a direction of rolling and show roughness that can have from a single to a double value respectively in the direction parallel to or the direction perpendicular to rolling (Fig. A4a). Thus, it appeared legitimate to question whether the shape of the drop is affected or not by the rolling direction. Fig. A5 shows that the drop is not deformed. In addition, ten measurements were made in each direction, and Fig. A4b shows that the contact angle varies little according to the direction of rolling with a value around 83°. The contact angle will, in what follows, always be measured in the direction perpendicular to rolling.
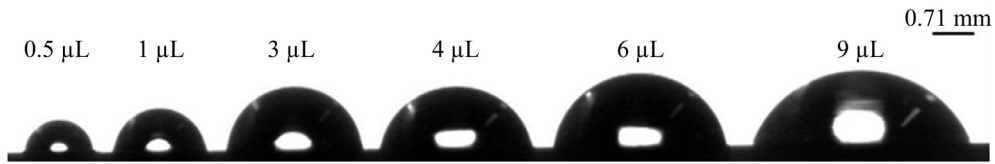
Fig. A2. Drop profiles in relation to the volume deposited on 1 mm rolled substrate AA 1050 degreased using acetone.
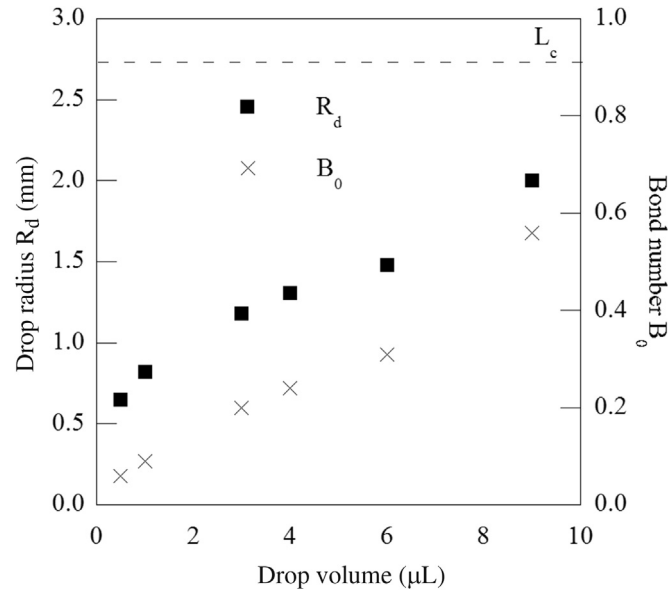

Fig. A3. Drop radius R_d and Bond number B_0 in relation to the drop volume on 1 mm rolled substrate AA 1050 degreased using acetone.
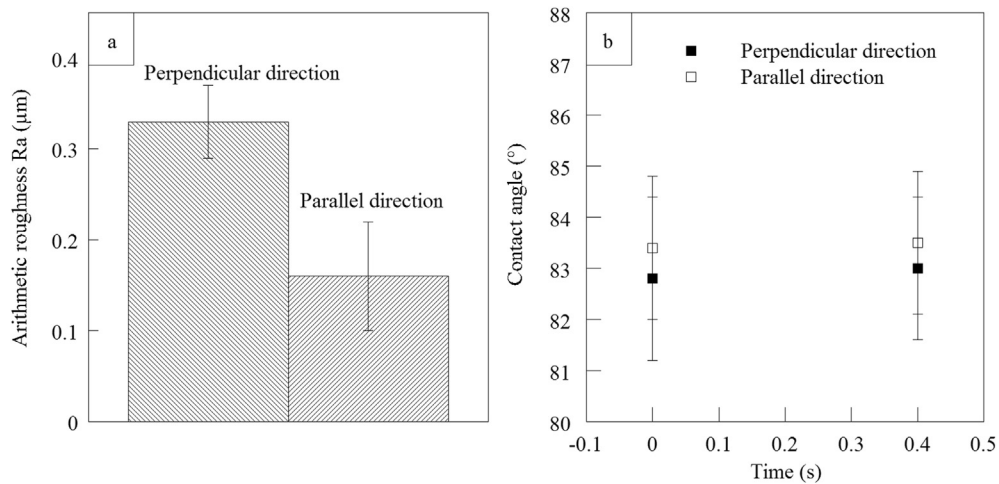

Fig. A4. (a) Arithmetic roughness Ra and (b) contact angle in relation to the direction of rolling on 1 mm rolled substrate AA 1050 degreased using acetone.
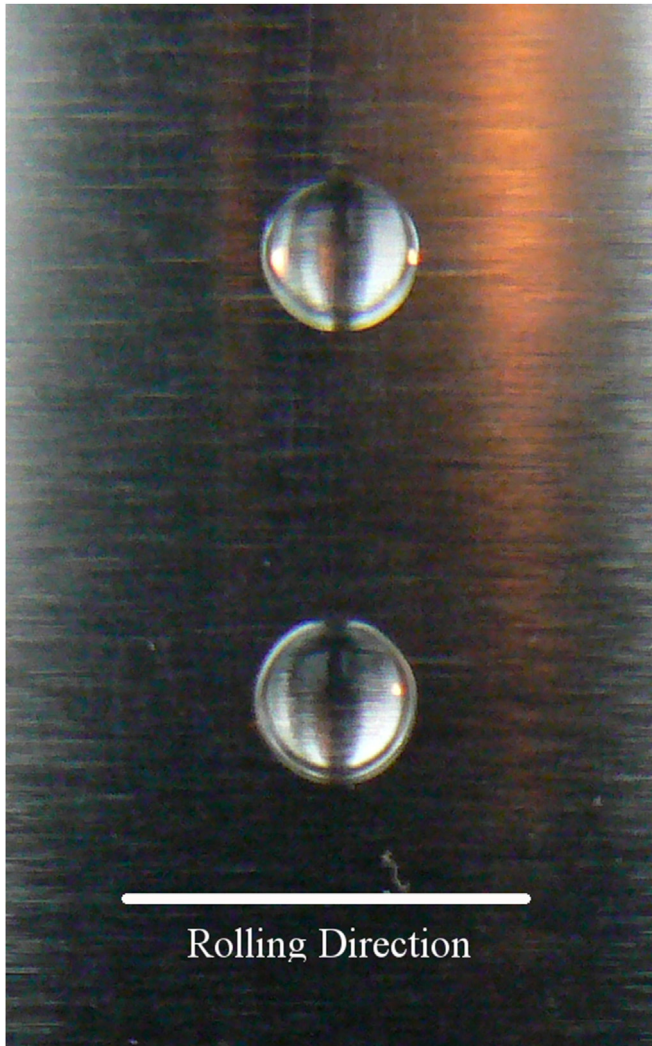
Fig. A5. Observation of drops with volume v = 4 μL, deposited on 1 mm rolled substrate AA 1050 degreased using acetone.

References

[1] Y. Yuan, T.R. Lee, Contact angle and wetting properties, in: G. Bracco, B. Holst (Eds.), Surface Science Techniques, Springer Series in Surface Science Techniques, 2013, pp. 3—34.

[2] X. Liu, Y. Liang, F. Zhou, W. Liu, Extreme wettability and tunable adhesion: biomimicking beyond nature? Soft Matter 8 (2012) 2070—2086.

[3] J.G. Buijnsters, R. Zhong, N. Tsyntsaru, J.-P. Celis, Surface wettability of macroporous anodized aluminum oxide, ACS Appl. Mater. Interfaces 5 (2013) 3224—3233.

[4] C. Ran, G. Ding, W. Liu, Y. Deng, W. Hou, Wetting on nanoporous alumina surface: transition between Wenzel and Cassie states controlled by surface structure, Langmuir 24 (2008) 9952—9955.

[5] V. Raspal, K.O. Awitor, C. Massard, E. Feschet-Chassot, R.S.P. Bokalawela, M.B. Johnson, Nanoporous surface wetting behavior: the line tension influence, Langmuir 28 (2012) 11064—11071.

[6] H. Leese, V. Bhurtun, K.P. Lee, D. Mattia, Wetting behaviour of hydrophilic and hydrophobic nanostructured porous anodic alumina, Colloids Surf. Physicochem. Eng. Asp. 420 (2013) 53—58.

[7] R. Redón, A. Vázquez-Olmos, M.E. Mata-Zamora, A. Ordóñez-Medrano, F. Rivera-Torres, J.M. Saniger, Contact angle studies on anodic porous alumina, J. Colloid Interface Sci. 287 (2005) 664—670.

[8] J.N. Mateo, S.S. Kulkarni, L. Das, S. Bandyopadhyay, G.C. Tepper, K.J. Wynne, S. Bandyopadhyay, Wetting behavior of polymer coated nanoporous anodic alumina films: transition from super-hydrophilicity to super-hydrophobicity, Nanotechnology 22 (2011), 035703 (10 pp).

[9] L. Yao, M. Zheng, L. Ma, W. Li, M. Li, W. Shen, Self-assembly of diverse alumina architectures and their morphology-dependent wettability, Mater. Res. Bull. 46 (2011) 1403—1408.

[10] J. Yang, J. Wang, C.-W. Wang, X. He, Y. Li, J.-B. Chen, F. Zhou, Intermediate wetting states on nanoporous structures of anodic aluminum oxide surfaces, Thin Solid Films 562 (2014) 353—360.

[11] P. Bares, C. Gazeau, C. Stephan, D. Pedelmas, C. Rossignol, S. Bruet et al., Procédé d'anodisation de pièces en alliage d'aluminium, Patent WO2013117759A1 (2013).

[12] K. Giffard, Etude des mécanismes de colmatage de films anodiques sur substrats d'aluminium aéronautiques, Thèse de doctorat de l'Université de Toulouse, 2015. (in French).

[13] N. Sobczak, M. Singh, R. Asthana, High-temperature wettability measurements in metal/ceramic systems — some methodological issues, Curr. Opin. Solid State Mater. Sci. 9 (2005) 241—253.

[14] H. Song, Y. Lee, S. Jin, H.-Y. Kim, J.Y. Yoo, Prediction of sessile drop evaporation considering surface wettability, Microelectron. Eng. 88 (2011) 3249—3255.

[15] Z. Li, J. Wang, Y. Zhang, J. Wang, L. Jiang, Y. Song, Closed-air induced composite wetting on hydrophilic ordered nanoporous anodic alumina, Appl. Phys. Lett. 97 (2010), 233107 (3 pp).

[16] M. Zheng, M. Sakairi, H. Jha, Influence of desiccation procedure on the surface wettability and corrosion resistance of porous aluminium anodic oxide films, Corros. Sci. 55 (2012) 332—338.

[17] W.B. Hardy, The spreading of fluids on glass, Lond. Edinb. Dublin Phil. Mag. J. Sci. 38 (1840) 49—55.

[18] E. Bormashenko, Y. Bormashenko, T. Stein, G. Whyman, R. Pogreb, Z. Barkay, Environmental scanning electron microscopy study of the fine structure of the triple line and cassie-wenzel wetting transition for sessile drops deposited on rough polymer substrates, Langmuir 23 (2007) 4378—4382.

[19] A. Marmur, Wetting on hydrophobic rough surface: to be heterogeneous or not to be, Langmuir 19 (2003) 8343—8348.

[20] M. Hilpert, B.-D. Avishai, Infiltration of liquid drops into porous media: effects of dynamic contact angle and contact angle hysteresis, Int. J. Multiph. Flow 35 (2009) 205—208.